Journal of the European Ceramic Society 21 (2001) 2487–2493

www.elsevier.com/locate/jeurceramsoc

Crystallization kinetics of mullite from Al_2O_3–SiO_2 glasses under non-isothermal conditions

Takahiro Takei[1], Yoshikazu Kameshima, Atsuo Yasumori, Kiyoshi Okada*

Department of Metallurgy and Ceramics Science, Graduate School of Science and Engineering, Tokyo Institute of Technology, O-okayama, Meguro Tokyo 152-8552, Japan

Abstract

The kinetics of mullite crystallization from Al_2O_3–SiO_2 glasses with chemical compositions ranging from 15 to 50 mol% Al_2O_3 were investigated under non-isothermal conditions using DTA. The glasses were prepared by ultra-quenching of molten droplets formed at the tip of a sintered aluminosilicate rod by an infra-red imaging furnace quenched by a twin-roller system. All the samples showed an exothermic peak at about 1000°C associated with mullitization. This crystallization temperature increased slightly with decreasing Al_2O_3 content. The exothermic peak split into two peaks at a glass composition of about 25 mol% Al_2O_3. This splitting is thought to be related to phase separation of the glass preceding mullitization. The activation energies for the nucleation-growth mechanism of mullitization, calculated by the Kissinger method, were 900–1300 kJ/mol, in good agreement with those for glass fibers obtained under isothermal conditions (Takei, T., Kameshima, Y., Yasumori, A. and Okada, K., Crystallization kinetics of mullite in alumina–silica glass fibers. *J. Am. Ceram. Soc.*, 1999, **82**, 2876–2880).

Keywords: Activation energy; Crystallization; DTA; Glass; Mullite

1. Introduction

Mullite ($Al_{4+2x}Si_{2-2x}O_{10-x}$) is the thermodynamically stable aluminosilicate at atmospheric pressure. It is a major crystalline phase in porcelain and plays an important role in increasing its mechanical strength. In recent years, mullite prepared from high purity synthetic raw materials has become a candidate as a high temperature structural ceramic because of its good mechanical strength and creep resistance at high temperatures.

Crystallization reactions of mullite from various raw materials have been reported by many workers. The crystallization process of mullite is divided into two types,[1] (1) direct crystallization from an amorphous phase which occurs when the precursor is homogeneous at the molecular level as in glass, monophasic gel[2] and slow hydrolysis (SH) gel,[3] and (2) crystallization via a spinel-phase which occurs when the precursor is inhomogeneous at the molecular level as in diphasic ge1[4–6] and rapid hydrolysis (RH) gel.[3] The activation energies (E_a) for nucleation-growth of mullitization from monophasic gels,[2] diphasic gels,[4–10] hybrid gels,[7] glass fibers[11] and kaolinites[12] have been examined by many workers using isothermal and/or non-isothermal methods. These reported data are summarized in Table 1. The reported E_a values from monophasic gels[2] and kaolinites[12] are about 300–530 kJ/mol[2] while those from diphasic gels,[4–10] hybrid gels[7] and glass fibers[11] are about 800–1300 kJ/mol, more than twice as large as for the former group. The differences in these E_a values may be due to the differences in the crystallization processes mentioned above, or to experimental conditions (e.g. firing temperature) and sample impurities, but the details are not yet fully understood.

Although the crystallization behavior of mullite from Al_2O_3–SiO_2 glasses has been reported by many workers,[13–15] little attention has been paid to the crystallization kinetics. We have, therefore, previously investigated the crystallization kinetics of mullite from glass fibers and measured the activation energies by an isothermal heating method.[11] The crystallization and growth of mullite could be described by three stages corresponding to nucleation, nucleation-growth and coalescence of mullite grains. The E_a values for three stages were 865–980, 1099–1288 and 645–696 kJ/mol, respectively. The E_a values for nucleation-growth of mullite from the glass fibers are, therefore, apparently

* Corresponding author.
E-mail address: kokada@ceram.titech.ac.jp (K. Okada).
[1] Present address: Institute of Inorganic Synthesis, Yamanashi University, 7 Miyamae, Kofu, Yamanashi 400-0021, Japan.

0955-2219/01/$ - see front matter
PII: S0955-2219(01)00266-7

Table 1
Reported activation energies for nucleation-growth of mullite from various starting materials

Starting material	Composition (mol% Al_2O_3)	Activation energy (kJ/mol)	Time exponent	Temperature range (°C)	Experimental condition	Reference
Diphasic gel	60.0	1070±200	1.3	1200–1300	XRD	Wei and Holloran (1988)[5]
Diphasic gel (0M)	61.4	1034±124	3.5	1200–1275	XRd	Wei and Holloran (1988)[5]
Hybrid gel (25M)	61.4	984±71	2.7	1200–1275	XRD	Wei and Holloran (1988)[5]
Hybrid gel (75M)	61.4	1091±71	1.6	1150–1225	XRD	Huling and Messing (1991)[7]
Hybrid gel (5M)	60.0	960±91	3.1	1200–1275	XRD	Huling and Messing (1991)[7]
Hybrid gel (10M)	58.6	932±49	3.3	1200–1275	XRD	Huling and Messing (1991)[7]
Diphasic gel	33.3	1080±63	–	1300–1390	DTA	Li and Thomson (1991)[8]
	50.0	892±48	–	1300–1390	DTA	Li and Thomson (1991)[8]
	60.0	1034±37	–	1300–1390	DTA	Li and Thomson (1991)[8]
	60.8	1108 ±44	–	1300–1390	DTA	Li and Thomson (1991)[8]
	75.0	1038 ±38	–	1300–1390	DTA	Li and Thomson (1991)[8]
TEOS-coated Al_2O_3	–	1042±32	–	–	–	Sacks et al. (1991)[9]
Diphasic gel	60.4	950±82	1.0	1200–1300	XRD	Lee and Yu (1992)[4]
	50.9	879±22	–	1270–1315	DTA	Lee and Yu (1992)[4]
	59.7	891±17	–	1275–1315	DTA	Lee and Yu (1992)[4]
	59.8	829±24	–	1265–1310	DTA	Lee and Yu (1992)[4]
	60.3	759±26	–	1255–1300	DTA	Lee and Yu (1992)[4]
	60.4	841±23	–	1275–1315	DTA	Lee and Yu (1992)[4]
	62.5	860±32	–	1275–1315	DTA	Lee and Yu (1992)[4]
	73.0	932±29	–	1275–1315	DTA	Lee and Yu (1992)[4]
Kaolinite (KGA-1)	33.3	523 ±34	–	1300–1400	High-temp.	Gualtieri et al. (1995)[12]
Kaolinite (KGA-2)	33.3	360±21	–	1300–1400		Gualtieri et al. (1995)[12]
Diphasic gel	60	880±30	–	1300–1400	DTA	Boccaccini et al. (1999)[10]
Glass fiber	36.1	1288±33	–	920–965	DTA	Boccaccini et al. (1999)[10]
	36.1	1195±31	–	1000–1200	XRD	Takei et al. (1999)[11]
	56.7	1138±29	–	920–965	XRD	Takei et al. (1999)[11]
	56.7	1099±44	–	1000–1200	XRD	Takei et al. (1999)[11]

larger than those of monophasic gels[2] which form mullite by the same process.

In the present paper, the activation energies for crystallization of mullite from Al_2O_3–SiO_2 glasses of various compositions were measured by a non-isothermal DTA method and the crystallization mechanisms are discussed in relation to the chemical composition.

2. Experimental procedures

2.1. Preparation of glasses by an ultra-quenching method

The glass samples were prepared by an ultra-quenching method using an arc image furnace and a twin-roller. The chemical compositions of the Al_2O_3–SiO_2 glasses were 15, 20, 25, 30, 36, 40, 50 and 60 mol% Al_2O_3, designated as R15, R20,. . .., respectively. The starting materials were tetraetylorthosilicate (TEOS: Wako Pure Chemicals) and aluminum nitrate nonahydrate (ANN: Wako Pure Chemicals). The appropriate amounts of TEOS and ANN were mixed in absolute ethanol with vigorous stirring for 3 h, and gelled slowly in an oven at 60°C for 1 month.[3] The resulting gels (SH gel) were calcined at 500°C for 6 h and 800°C for 24 h to remove organic matter. The powder was pressed into a rod by CIP at 98 MPa and sintered at 1300°C for 12 h.

The tip of the sintered rod was melted at 2100°C using an arc image furnace (NEC Model FQ-50XS) and the molten droplet was ultra-quenched by dropping through a twin-roller rotating at 1500 rpm. The resulting samples were transluscent and flaky (with the exception of the 60 mol% sample). The estimated quenching rate by this method is greater than 10^5 K/s.[16]

2.2. Activation energy by the Kissinger method

To investigate the crystallization mechanism of mullite from the glasses, the DTA curves were measured (Rigaku TG-8 120) at heating rates of 1, 2, 5 and 10°C/min. The activation energy for nucleation-growth of mullite was calculated from the exothermic DTA peak using the Kissinger equation[17] as follows:

$$\ln\left(\frac{\alpha}{T_0^2}\right) = -\frac{E_a}{RT_0} + C,$$

where α is the heating rate, E_a is the activation energy for nucleation-growth of mullite, R is the gas constant, T_0 is the exothermic peak temperature and C is a constant. Augus and Bennet[18] and Ray et al.[19] reported that the crystallization mechanism could be determined from the shape factor (n) of the exothermic peak represented by the following equation:

$$n = \frac{2.5}{\Delta T}.\frac{T_0^2}{(E_a/R)},$$

where n is called the Avrami constant and ΔT is the full width at half maximum of the exothermic peak. Here, smaller n values indicate that the crystallization is dominated by a surface crystallization mechanism rather than by volume crystallization, and/or that the crystallization dimension is low. On the other hand, larger n values are expected only in case of increasing nucleation rates, i.e. >2.5 in diffusion controlled reaction or >4 in polymorphic transformation.

The crystalline phases formed in the as-quenched and annealed glasses were determined by powder X-ray diffractometry (XRD) using monochromated CuK_α radiation (Rigaku Geigerflex). Microstructures of the samples were observed by a Field-Emission type scanning electron microscope (FE-SEM, Jeol JCM890-S).

3. Results

3.1. Crystallization of glasses

The XRD patterns of the ultra-quenched glasses are shown in Fig. 1. These patterns show only a halo, with no diffraction peaks of mullite except in the R60 sample. The samples R15–R50 were, therefore, confirmed to be fully vitrified. The positions of their halos shifted to higher reflection angles and their heights decreased with increasing Al_2O_3 content. These changes may be caused by variation in the interatomic distances and in the short-range ordering of the glasses.

The crystallization of glass can occur either from the surface or uniformly in the bulk. In order to investigate the crystallization mechanism of mullite in the present glasses, the fractured surfaces of sample R50 before and after annealing at 900°C were observed by FE–SEM. Fig. 2(a) and (b) shows the XRD patterns and SEM micrographs of the fractured surfaces of R50, as-quenched and annealed at 900°C for 12 h, respectively. The amount of mullite in the sample annealed for 12 h was evaluated from the integrated intensity ratio of the 121 diffraction peaks of the 12 and 48 h annealed samples. The fraction of mullite in the 12 h annealed sample was about 0.38. If mullite crystallized from the surface, it would be expected to form a surface layer 5–6 μm thick, on the basis of the measured mullite fraction in this

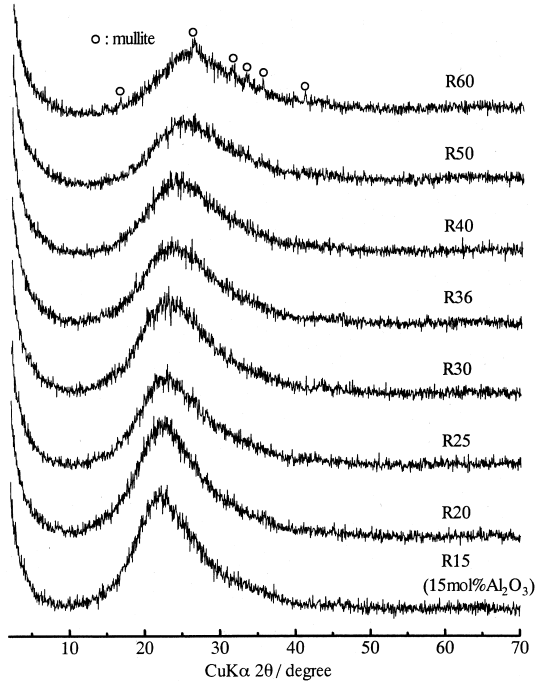

Fig. 1. XRD patterns of ultra-quenched Al_2O_3–SiO_2 glasses with various compositions.

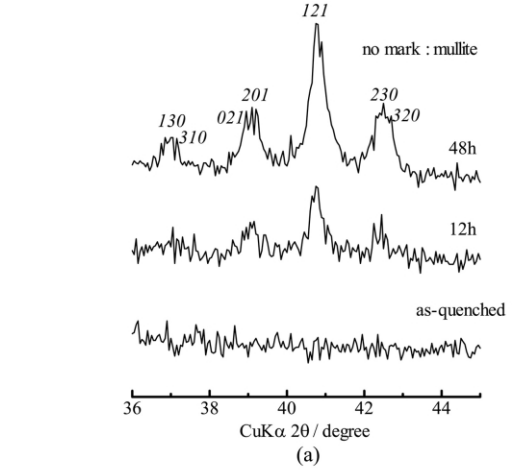

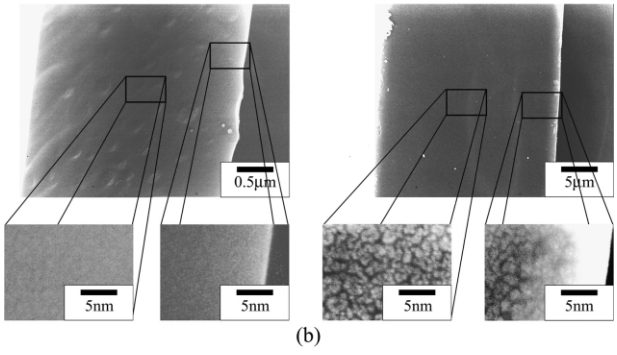

Fig. 2. (a) XRD patterns of R50 as-quenched and annealed at 900°C for 12 and 48 h (left), (b) FE–SEM photographs of fractured surfaces of R50 as-quenched and annealed at 900°C for 12 h (right).

sample. The SEM photographs of the fractured surfaces [Fig. 2(a) and (b)] show a mullitization texture in all the fractured areas, suggesting that mullite crystallization in the present glasses occurs by volume crystallization and not by surface crystallization. This result is consistent with that found for glass fibers.[11]

3.2. Activation energy

The DTA curves of the glasses measured at a heating rate of 5°C/min are shown in Fig. 3. Exothermic peaks were observed at about 1000°C in all samples, the temperatures tending to decrease slightly with increasing Al_2O_3 content. The exothermic peak corresponding to mullitization was not observed in R15 because the Al_2O_3 content in this sample is too low. Single exothermic peaks were observed in R20, R40 and R50, whereas the thermal events in R25, R30 and R36, especially R25, were doublets. The peaks appearing at the lower and higher temperatures are designated *l*-peaks and *h*-peaks, respectively. The temperatures of the *l*-peaks were almost constant while those of the *h*-peaks increased with decreasing Al_2O_3 content. These exothermic peaks merge into a single peak in the Al_2O_3-rich glasses R40 and R50. The cause of this peak separation and temperature shift will be discussed below.

Fig. 4 shows the DTA curves of R25 and R40 determined at heating rates of 1, 2, 5 and 10°C/min. The top temperatures of these exotherms increase with increasing heating rate. From these data, a Kissinger plot [$\ln(\alpha T_0^{-2}]$ vs T^{-1}) was obtained for each sample as shown in Fig. 5. The activation energies (E_a) for nucleation-growth of mullite in these samples were evaluated from the plots. Table 2 shows the resulting E_a values and Avrarni constants (n) of these samples. For R25, two activation energies, E_a^L and E_a^H, were obtained from the *l*- and *h*-peaks, respectively. Although R30 and R36 showed a doublet peak shape, their poor resolution

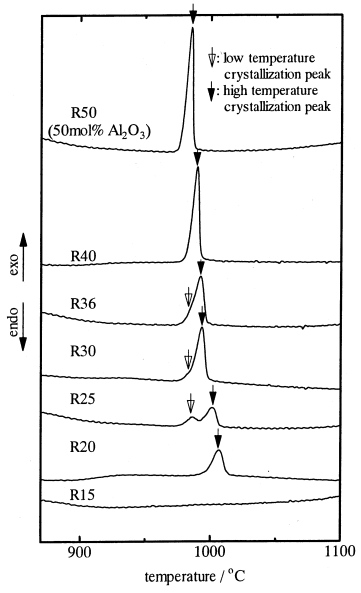

Fig. 3. DTA curves of ultra-quenched Al_2O_3–SiO_2 glasses with various compositions.

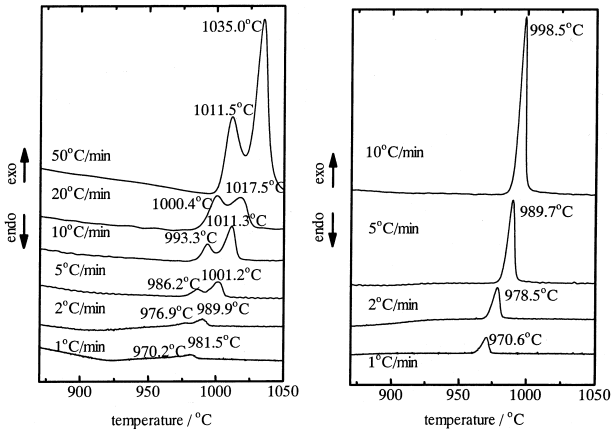

Fig. 4. DTA curves of ultra-quenched Al_2O_3–SiO_2 glasses measured at various heating rates: (a) R25 and (b) R40.

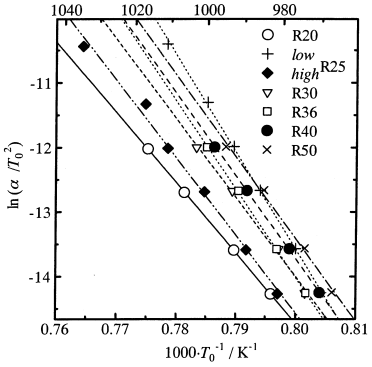

Fig. 5. Kissinger plots of ultra-quenched Al_2O_3–SiO_2 glasses with various compositions.

Table 2
Activation energies (E_a) for nucleation-growth of mullite from various Al_2O_3–SiO_2 glasses calculated by the Kissinger method

Composition (mol% Al_2O_3)	20	25	30	36	40	50
E_a^L (kJ/mol)[a]	–	1281±19	–	–	–	–
E_a^H (kJ/mol)[b]	903±4	1019±42	1015±46	1133±13	1062±12	1052±53
Avrami constant	3.5–3.9	–	4.0–4.5	3.3–3.9	5.0–5.9	5.6–7.1

[a] Activation energy calculated from the *l*-peak of exothermic peak.
[b] Activation nergy calculated from the *h*-peak of exothermic peak.

made it difficult to obtain two separate E_a values; the E_a^H values of these samples, therefore, include both contributions. The calculated E_a^H reached its maximum value in R36 but the variation with chemical composition is quite small. The E_a^L value in R25 is greater than E_a^H. The resulting Avrami constants, *n,* were about 3–7, consistent with a volume crystallization mechanism in these glasses and also suggest that the mullite crystallization may proceed with increasing nucleation rate.

4. Discussion

4.1. Splitting of the DTA exothermic peak

As shown in Figs. 3 and 4, the DTA exothermic peak of R25 is split into two peaks. Similar peak splitting was also reported by Okada and Ostuka[3] in the Al_2O_3–SiO_2 SH gels with a similar range of compositions, although they did not explain the cause of the peak splitting. Since no peak splitting was observed in the RH gels even of the same compositions,[3] this phenomenon is only observed in samples which show direct mullitization at about 1000°C. From these results, we suggest that the splitting of the DTA exotherm may be related to immiscible phase separation which is known to occur rapidly by spinodal decomposition even in rapidly quenched samples such as the present as-quenched glasses. Here, the composition of R25 corresponds to the known spinodal region in the Al_2O_3–SiO_2. system.[20] The doublet exothermic peak may, therefore, correspond to mullitization from two phase separated regions with the Al_2O_3-rich and SiO_2-rich compositions. To confirm this hypothesis, sample R25 was heated to 1000 and 1025°C under the same conditions in the DTA. These temperatures occur just after the *l*- and *h*-peaks in the DTA curve shown in Fig. 6. Fig. 7 shows the XRD patterns of the as-quenched, 1000° and 1025°C R25 samples. The amount of mullite in the 1025°C sample has increased with respect to the 1000°C sample, suggesting that both DTA exotherms are due to mullite crystallization. The slightly different mullitization temperatures correspond to crystallization from two phase-separated phases.

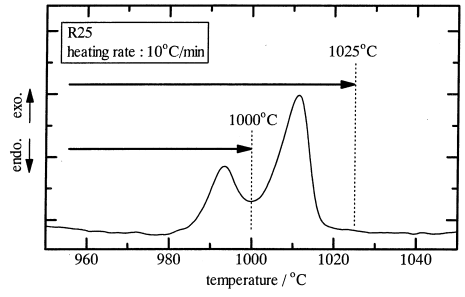

Fig. 6. DTA exothermic peaks observed in R25 and the corresponding heat treatment temperatures.

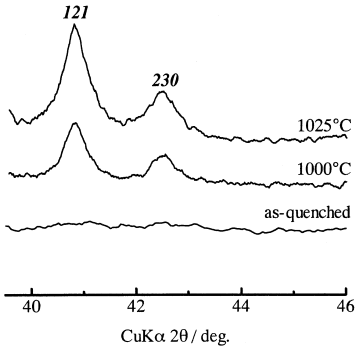

Fig. 7. XRD patterns of R25 as-quenched, heated at 1000 and 1025°C.

The compositions of Al_2O_3- and SiO_2-rich phases in the phase-separated texture were determined to be about 60 and 10 mol% Al_2O_3, respectively, from the reported immiscibility region[2]. Since the composition of the Al_2O_3-rich phase is close to that of mullite, the diffusion path length required for its mullitization should be very short. On the other hand, this length will be much longer in the SiO_2-rich phase in which the composition is very different from that of mullite, making mullitization more dependent on the transport of cations and anions. Mullite should therefore crystallize from the Al_2O_3-rich phase before the SiO_2-rich phase. Thus, the onset temperature for mullitization is almost constant in glass compositions from 50 to 25 mol% Al_2O_3 because the composition of the Al_2O_3-rich phase is same for all the phase separated glasses. Moreover, the temperature of mullitization from the SiO_2-rich phase increases because the diffusion path length for mullitization increases with decreasing Al_2O_3 content. Since the SiO_2-rich phase is surrounded by the mullite grains already formed from the Al_2O_3-rich phase, its crystallization temperature should depend on the volume fraction of the mullite already formed. This should lead to an increase in the mullitization temperature with decreasing Al_2O_3 content, as is observed from the DTA exotherm temperatures shown in Fig. 3.

4.2. Aclivation energy

The E_a values for nucleation-growth of mullite from the glasses calculated from the DTA curves using the Kissinger equation are shown in Table 2. These E_a values are in good agreement with those obtained for glass fibers under isothermal conditions,[11] listed in Table 1. The mechanism of mullitization from glasses was investigated in detail using the E_a values of Table 2. The activation energy of the *l*-peak (E_a^L) was 1281 kJ/mol whereas those of the *h*-peaks (E_a^H) ranged from 903 to 1133 kJ/mol. On the basis of the above discussion, E_a^L is attributed to mullitization from the Al_2O_3-rich phase and E_a^L to mullitization from both phases. In general, E_a^L should

be smaller than E_a^H. However, the present E_a^L value is rather larger than E_a^H. This conflicting result can be reasonably be resulted as follows. Mullitization from the Al_2O_3-rich phase is considered to start by heterogeneous nucleation from sites which may be located at interfaces between the Al_2O_3-rich and SiO_2-rich phases in the phase separated glasses. On the other hand, mullitization from the SiO_2-rich phase also occurs by heterogeneous nucleation at sites in the interfaces between already formed mullite grains and the amorphous SiO_2-rich phase. Since the interface energy between the Al_2O_3-rich and SiO_2-rich phases is considered to be much smaller than between mullite and the SiO_2-rich phase, mullitization which occurs at lower temperature from the Al_2O_3-rich phase will have a greater activation energy than the higher temperature reaction in the SiO_2-rich phase.

We have previously reported the mechanism of mullitization from Al_2O_3–SiO_2 glass fibers under isothermal conditions.[11] Mullite formation occurred in two steps, increasing steeply in the temperature range of 900–950°C with a plateau at 950–1050°C followed by a gentle increase at >1050°C. We divided these two-step curves into 1st, 2nd and 3rd stages and concluded that nucleation predominantly occurred in the 1st stage, nucleation-growth became dominant in the 2nd stage and coalescence of mullite grains dominated in the 3rd stage. The E_a values for nucleation-growth of mullite $\left(E_a^{NG}\right)$ in the 1st and 2nd stages were about 1150–1300 and 1100–1200 kJ/mol, respectively. The E_a^L value of about 1300 kJ/mol is associated with mullitization from the Al_2O_3-rich phase in phase separated R25 glass whereas the E_a^H values of about 900–1100 kJ/mol relate to both the Al_2O_3- and SiO_2-rich phases in all samples except R25. Since mullitization can occur from the Al_2O_3-rich phase without distinct variation in the composition, nucleation may be the dominating mechanism. On the other hand, since mullitization in the other samples is associated with both the SiO_2- and Al_2O_3-rich phases, and requires ion transport, a nucleation-growth mechanism dominates this stage because the diffusion of ions is required for the growth of mullite crystals. In fact, the present E_a^L and E_a^H values are in good agreement with the previous values of E_a^{NG} for the 1st and 2nd stages in the glass fibers, and are thus considered to correspond to the E_a^{NG} of the 1st and 2nd stages of the previous results.[11]

Al_2O_3–SiO_2 glasses are seen to have E_a values 1000 kJ/mol for nucleation-growth of mullite. These Eavalues are similar to those reported in diphasic gels[4–10] and hybrid gels[7] but are much higher than those of monophasic gels[2] and kaolinites.[12] Since the mullitization temperatures are lower in glasses and monophasic gels than in diphasic gels, hybrid gels and kaolinites, there is no clear correlation between the mullitization temperature and E_a for nucleation-growth of mullite in these starting materials. The kaolinite starting materials referred to were from Georgia (Kga-1 and Kga-2), and are known to contain relatively high TiO_2 impurity levels (1–2 mass%),[21] which generally provides heterogeneous nucleation sites and accelerates the phase transition[22] and crystallization of glasses.[23] it may be possible that the low E_a values reported in the kaolinites are largely due to this accelerating effect of TiO_2. In the previous work on monophasic gels, Li and Thomson[2] obtained the E_a values for mullite nucleation and not for nucleation-growth. It may be, therefore, inappropriate to directly compare their E_a values with the present values for mullite nucleation-growth. Further, in their analysis of E_a for the monophasic gels, they did not use the conventional Avrami equation, which may be also contribute to the differences in their E_a values compared with other workers. If it is accepted that the E_a values reported for the monophasic gels and kaolinites are exceptional cases, all the other E_a values for nucleation-growth of mullite from various starting materials are about ≈11000 kJ/mol, irrespective of their mullitization temperatures.

This unusual result is contrary to the general trend of the lower the temperature the lower the E_a.[22]

5. Conclusion

The crystallization kinetics of mullite in Al_2O_3–SiO_2 glasses were determined by DTA under non-isothermal conditions, with the following results.

1. Mullite formation from the present glasses proceeds by a volume crystallization mechanism rather than by surface crystallization.
2. Exothermic DTA peaks were attributed to crystallization of mullite. In glasses with compositions corresponding to the region of immiscibility phase separation, the DTA exotherm peak is split into two peaks which may overlap. These correspond to mullitization from Al_2O_3- and SiO_3-rich phase in the phase separated glasses.
3. The activation energies obtained from the DTA curves range from about 900 to 1300 kJ/mol and show good agreement with values for nucleation-growth of mullite from glass fibers under isothermal conditions[11] and with other starting materials such as diphasic gels[4–10] and hybrid gels.[7]

Acknowledgements

The authors are grateful to Dr. K.J.D. MacKenzie of The New Zealand Institute for Industrial Research and Development for editing and fruitful suggestions to the manuscript.

References

1. Schneider, H., Okada, K. and Pask, J. A., *Mullite and Mullite Ceramics*. John Wiley & Sons, New York, 1994.
2. Li, D. X. and Thomson, W. J., Mullite formation kinetics of a single-phase gel. *J. Am. Ceram. Soc.,* 1990, **73**, 964–969.
3. Okada, K. and Otsuka, N., Characterization of the spinel phase from SiO_3–Al_2O_3 xerogels and the formation process of mullite. *J. Am. Ceram. Soc.,* 1986, **69**, 652–656.
4. Lee, J. S. and Yu, S. C., Mullite formation kinetics of coprecipitated Al_2O_3–SiO_2 gels. *Mater. Res. Bull.,* 1992, **27**, 405–416.
5. Wei, W. C. and Halloran, J. W., Transformation kinetics of diphasic aluminosilicate gels. *J. Am. Ceram. Soc.,* 1988, **71**, 581–587.
6. Li, D. X. and Thomson, W. J., Kinetics mechanism for mullite formation from sol-gel precursors. *J. Mater. Res.,* 1990, **5**, 1963–1969.
7. Huling, J. C. and Messing, G. L., Epitactic nucleation of spinel in aluminosilicate gels and its effect on mullite crystallization. *J. Am. Ceram. Soc.,* 1991, **74**, 2374–2381.
8. Li, D. X. and Thomson, W. J., Mullite formation from non-stoichiometric diphasic precursors. *J.Am. Ceram. Soc.,* 1991, **74**, 2382–2387.
9. Sacks, M. D., Bozkurt, N. and Scheiffele, G. W., Fabrication of mullite and mullite-matrix composites by transient viscous sintering of composite powders. *J. Am. Ceram. Soc.,* 1991, **74**, 2428–2437.
10. Boccaccini, A. R., Khalil, T. K. and Bucker, M., Activation energy for the mullitization of a diphasic gel obtained from fumed silica and boehmite sol. *Mater. Lett.,* 1999, **38**, 116–120.
11. Takei, T., Kameshima, Y., Yasumori, A. and Okada, K., Crystallization kinetics of mullite in alumina–silica glass fibers. *J. Am. Ceram. Soc.,* 1999, **82**, 2876–2880.
12. Gualtieri, A., Bellotto, M., Artioli, G. and Clark, S. M., Kinetic study of the kaolinite–mullite reaction sequence. Part II: mullite formation. *Phys. Chem. Miner.,* 1995, **22**, 215–222.
13. Macdowell, J. F. and Beall, G. H., Immiscibility and crystallization in Al_2O_3–SiO_2 glasses. *J. Am. Ceram. Soc.,* 1969, **52**, 17–25.
14. Ganz, R. and Krönert, W., Crystallization behaviour of high temperature ceramic fibers of the Al_2O_3–SiO_2 glasses. *Interceram.,* 1982, **31**, 136–144.
15. Ootsuka, T., Hamano, K., Tsutsumi, K. and Kurano, M., Crystallization of Al_2O_3–SiO_2 glass fiber and effect of ZrO_2 and Cr_2O_3 additions on the crystallization. *J. Ceram. Soc. Japan,* 1996, **104**, 301–307.
16. Chen, H. S. and Miller, C. E., A rapid quenching technique for the preparation of thin uniform films of amorphous solids. *Rev. Sci. Inst.,* 1970, **41**, 1237–1238.
17. Kissinger, H. E., Reaction kinetics in differential thermal analysis. *Anal Chem.,* 1957, **29**, 1702–1706.
18. Augis, J. A. and Bennet, J. E., Calculation of the Avrami parameters for heterogeneous solid state reactions using a modification of the Kissinger method. *J. Them. Anal.,* 1978, **13**, 283–292.
19. Ray, C. S., Yang, Q., Huang, W.-H. and Day, D. E., Surface and internal crystallization in glasses as determined by differential thermal analysis. *J. Am. Ceram. Soc.,* 1996, **49**, 3155–3160.
20. Takei, T., Kameshima, Y., Yasumori, A. and Okada, K., Calculation of metastable immiscibility region in the Al_2O_3–SiO_2 system using molecular dynamics simulation. *J. Mater. Res.,* 2000, **15**, 186–193.
21. Okada, K., Kawashima, H., Saito, Y., Hayashi, S. and Yasumori, A., New preparation method of mesoporous gamma-alumina by selective leaching of calcined kaolin minerals. *J. Mater. Chem.,* 1995, **5**, 1241–1244.
22. Okada, K., Hattori, A., Taniguchi, T., Nukui, A. and Das, R. N., Effects of divalent cation additives on the γ-Al_2O_3–αAl_2O_3 phase transition. *J. Am. Ceram, Soc.,* 2000, **83**, 928–932.
23. Lewis, M. H., ed., *Glasses and Glass-Ceramics*. Chapman and Hall, New York, 1989.